SCIENTIFIC REPORTS

OPEN

SUBJECT AREAS:
MATERIALS CHEMISTRY
SYNTHESIS
MATERIALS SCIENCE
BIOMATERIALS

Received
27 September 2012

Accepted
29 October 2012

Published
11 December 2012

Correspondence and requests for materials should be addressed to A.L.M.R. (leela@rice.edu); G.J. (john@sci.ccny.cuny.edu) or P.M.A. (ajayan@rice.edu)

# Lithium storage mechanisms in purpurin based organic lithium ion battery electrodes

Arava Leela Mohana Reddy[1], Subbiah Nagarajan[2], Porramate Chumyim[1], Sanketh R. Gowda[1], Padmanava Pradhan[2], Swapnil R. Jadhav[2], Madan Dubey[3], George John[2] & Pulickel M. Ajayan[1]

[1]Department of Mechanical Engineering and Materials Science, Rice University, Houston, TX 77005, USA, [2]Department of Chemistry, The City College of the City University of New York, New York, NY 10031, [3]U.S. Army Research Laboratory, 2800 Powder Mill Rd, Adelphi, MD 20783, USA.

**Current lithium batteries operate on inorganic insertion compounds to power a diverse range of applications, but recently there is a surging demand to develop environmentally friendly green electrode materials. To develop sustainable and eco-friendly lithium ion batteries, we report reversible lithium ion storage properties of a naturally occurring and abundant organic compound *purpurin*, which is non-toxic and derived from the plant *madder*. The carbonyl/hydroxyl groups present in purpurin molecules act as redox centers and reacts electrochemically with Li-ions during the charge/discharge process. The mechanism of lithiation of purpurin is fully elucidated using NMR, UV and FTIR spectral studies. The formation of the most favored six membered binding core of lithium ion with carbonyl groups of purpurin and hydroxyl groups at C-1 and C-4 positions respectively facilitated lithiation process, whereas hydroxyl group at C-2 position remains unaltered.**

The fundamental challenge in developing clean energy is to identify sustainable energy supplies and protect the environment[1–3]. Energy storage is a key component in this energy conversion-storage-delivery chain. Among various electrochemical energy storage options, lithium ion batteries have drawn utmost attention due to their reversible electrochemistry and superior gravimetric and volumetric energy storage capacities[4–6]. Research on lithium-ion battery (ever since its discovery in 1991 by Sony) was directed mainly towards the synthesis of high capacity materials and lead to the development of several non-renewable cathodes like $LiCoO_2$, $LiNiO_2$, $Li_2MnO_4$, $LiFePO_4$ *etc.*[7–10]. Current Li-ion battery technologies operating on inorganic insertion compound (e.g., $LiCoO_2$) as cathode, face severe safety issues and 30% of globally produced cobalt is channeled into battery technology[11]. Also, extracting raw materials from ores and transforming them into electrochemically active material requires increasing amounts of energy as they become scarcer. Further, recycling of current lithium ion batteries has become a very challenging process as it involves elevated temperatures and liberates high amounts of $CO_2$[4]. Energetically expensive fabrication/recycling process of current lithium ion battery technology is not viable in the long term and hence, lithium ion battery industry demands environment friendly green organic electrodes.

Early efforts on lithium battery built from organic cathode materials (polyaniline), met with limited success owing to numerous drawbacks such as, temperature stability, limited rate capability (low power density) and low specific and volumetric energy density[12–20]. Recently, Tarascon and co-workers suggested an innovative step towards the development of organic electrode materials through an elegant process[4]. Their recent work on conjugated dicarboxylate anodes and lithium salt of tetrahydroxybenzoquinone suggested a possible alternative to current inorganic based electrodes[21–23]. Recent research on biobased materials demonstrated the prudent use of biomass for value-added chemicals and products in a biorefinery concept[24,25]. Here, we report a novel organic electrode material for lithium ion batteries, *purpurin*, which has been extracted from a common plant *Madder*, most often used as a dye for fabrics. The extracted and chemically lithiated purpurin (CLP), shows very good reversible lithium ion storage properties. Hence, it could lead to the development of a green and sustainable Li ion battery.

## Results

To realize the reversible electrochemical performance of this novel electrode material, a working electrode was prepared by mixing 80% of purpurin/CLP and 20% of carbon by weight. Figure 1 (a) shows the cyclic

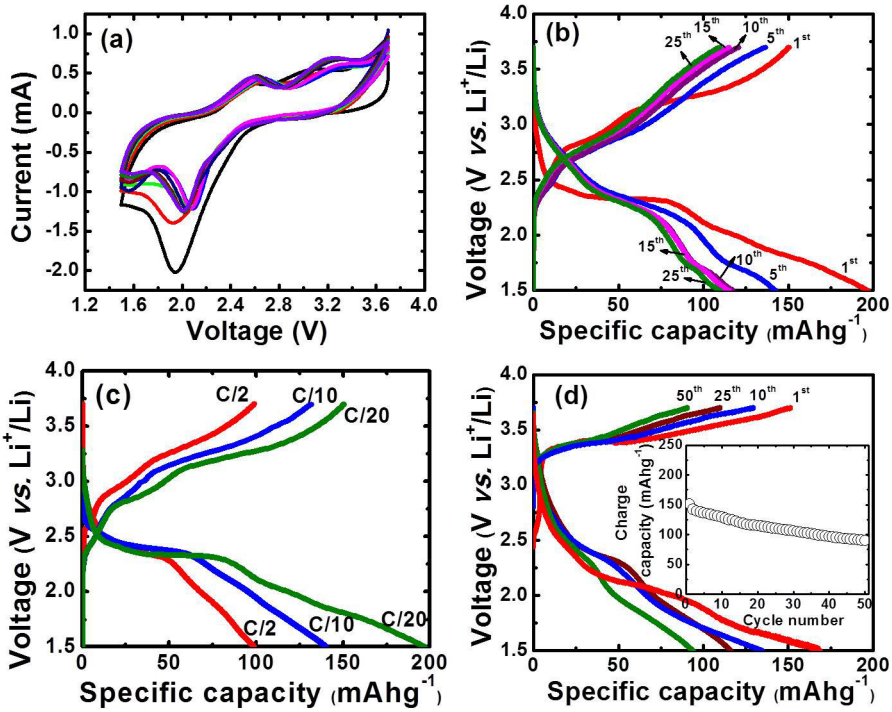


**Figure 1** | (a) Cyclic voltammograms of purpurin electrode in 1 M solution of $LiPF_6$ in 1 : 1 (v/v) mixture of ethylene carbonate (EC) and dimethyl carbonate (DMC) as the electrolyte with Li as counter and reference electrode (scan rate: 0.1 $mVs^{-1}$). (b) Voltage *vs* specific charge-discharge capacity of purpurin electrode cycled at a C/20 rate between 3.7 V and 1.5 V *vs* $Li/Li^+$ in 1 M solution of $LiPF_6$ in 1 : 1 (v/v) mixture of ethylene carbonate (EC) and dimethyl carbonate (DMC) as the electrolyte. (c) The voltage profiles of purpurin at different current rates (C/2, C/10 and C/20). The first charge/discharge curves are presented in the plot and (d) Voltage *vs* specific charge-discharge capacity of CLP electrode cycled at a C/20 rate between 3.7 V and 1.5 V *vs* $Li/Li^+$ in 1 M solution of $LiPF_6$ in 1 : 1 (v/v) mixture of ethylene carbonate (EC) and dimethyl carbonate (DMC) as the electrolyte. *Inset:* Variation in discharge capacity *vs* cycle number for the CLP electrode.

voltammogram of the purpurin electrode conducted at scan rate of 0.1 $mVs^{-1}$ in 1 M solution of $LiPF_6$ in 1 : 1 (v/v) mixture of ethylene carbonate (EC) and dimethyl carbonate (DMC) as an electrolyte against Li metal as counter and reference electrode. The cyclic voltammogram measurement of the purpurin electrodes showed reversible lithiation/de-lithiation process in purpurin molecule. The first cathodic scan showed a peak around ~2 V. As it can be observed from the cathodic scan of the cyclic voltammogram the lithiation process begins at 2.4 V and becomes quite large at ~2.0 V. The first anodic scan shows two small peaks around ~2.6 and 3.2 V respectively, associated with the de-lithiation process of purpurin. In the following scans of the cyclic voltammogram, the peaks of the cathodic scan shifts to the right by ~0.2 V, hence reducing the hysteresis between the anodic and cathodic peaks. This leads to better reversibility of the electrode around ~2.0 V.

After understanding the actual lithiation and de-lithiation potentials of the purpurin molecules from cyclic voltammogram measurements, another test cell was constructed and tested for their electrochemical performance in Li half-cells. Galvanostatic charge/discharge measurements were conducted between 3.7 V and 1.5 V *vs* $Li/Li^+$, with purpurin (80%)/Carbon (20%) as the working electrode. Figure 1(b), the voltage *vs* specific capacity plots conducted at C/20 rate between 3.7 V and 1.5 V *vs* $Li/Li^+$, clearly indicate a typical Li lithiation/de-lithiation behavior. During the first discharge, an initial drop in the potential to 2.5 V is observed and then a stable plateau occurs between 2.5 V and 2.3 V before dropping to 1.5 V. A first discharge capacity of ~196 mAh/g is observed. Upon recharge, de-lithiation of purpurin takes place in two steps observed in the form of two plateau regions from 2.2 V to 2.7 V and 2.7 V to 3.3 V. Thus the observed charge/discharge behavior from galvanostatic measurement is in good agreement with cyclic voltammogram measurements. The capacity loss in the subsequent cycles is attributed to irreversible process[6]. Further, galvanostatic charge/discharge experiments were conducted at various currents (C/2 and C/10) to investigate the rate capability of the electrode material. The comparative specific capacity *vs* voltage (first cycle of discharge/charge) profiles of purpurin at current rates of C/2, C/10 and C/20 are shown in Figure 1(c). The contour of the voltage *vs* specific capacity curve at higher current rates of C/2 is very similar to the one obtained at lower current rates. The discharge capacity of the first discharge cycle at a current rate of C/20 is much higher than that of C/10 and C/2. The decrease in specific capacity at higher current rates is due to poor electron conductivity of purpurin molecule. We have also compared the battery performance of pristine purpurin molecules with that of CLP by constructing another cell with CLP (80%)/carbon (20%) as working electrode. The voltage *vs* specific capacity plots conducted at C/20 rate between 3.7 V and 1.5 V *vs* $Li/Li^+$ shown in Figure 1(d), clearly indicates a typical lithiation/de-lithiation behavior in CLP molecules. The CLP electrode shows a reversible capacity of 90 mAh/g after 50 cycles of charge/discharge as observed in the capacity *vs* cycle number plot in *inset* of Figure 1(d). Changes in surface morphology of electrode material after several cycles of charge/discharge are observed using scanning electron microscopy (See Supporting information Figure S1).

The possible sequence of lithiation/de-lithiation mechanism in the purpurin molecule is schematically represented in figure 2 (a). From figure 2, (1) Molecular structure of pristine purpurin and corresponding hydrogen were labeled as $H_a$–$H_h$ respectively. Possible lithium binding core in purpurin is shown by orange color circles; (2) Possible reversible intermediate of lithiated purpurin and (3) Binding of lithium ion with carbonyl groups of purpurin and hydroxyl groups at C-1 ($-OH_a$) and C-4 ($-OH_c$) respectively.


**Figure 2** | (a) Schematic illustration of sequence of lithiation/de-lithiation mechanism in the purpurin molecule: (1) Molecular structure of pristine purpurin; (2) Intermediate of lithiated purpurin, and (3) Binding of lithium ion with carbonyl and hydroxyl groups of purpurin at C-1 ($-OH_a$) and C-4 ($-OH_c$) respectively. (b) Photograph of (1) pristine purpurin and (2) Chemically lithiated purpurin (1 : 2 ratio).

Upon lithiation of purpurin, existence of different forms of molecular structures, 1–3 are proposed based on detailed NMR spectral analysis of the lithiated purpurin electrode (ELP) as well as CLP, and were supported by UV-vis and FTIR studies. Figure 2 (b) Photograph of (1) Pristine purpurin and (2) Chemically lithiated purpurin (1 : 2 ratio). Further, to understand the electrochemical reaction mechanism between purpurin and lithium, NMR, FTIR, UV and XPS measurements were carried out on ELP and compared the obtained spectra with that of pristine purpurin. The $^{1}H$, $^{13}C$ and $^{7}Li$ NMR spectral data of CLP, where LiOAc acted as source for Li ions, are in good agreement with the electrochemically modified system (Figure 3, Figure 4, Figure S2 and Figure S3). NMR studies clearly depict the binding of $Li^+$ ions with carbonyls and simultaneously with the nearby hydroxyl groups of purpurin (Figure 2).

A careful examination of the $^{1}H$- and $^{13}C$-DEPT-135 NMR data in DMSO-$d_6$ clearly indicates the nature and extent of lithium incorporation into purpurin. $^{1}H$-NMR of the pristine purpurin showed multiplets at δ 7.8–8.1 ppm for the C-ring, a singlet at δ 6.58 ppm for the A-ring proton and singlets for the hydroxyl groups at δ 13.30, 13.05 and 11.57 ppm (Figure 3a). The broad singlet at δ 11.57 ppm was assigned to the phenolic hydroxyl groups ($H_b$), as it was broad due to weak intra-molecular H-bonding and chemical exchange. The $^{1}H$ NMR of ELP-1 and of pristine purpurin, were found to be similar except for the phenolic hydroxyl groups ($H_a$, $H_b$ and $H_c$) and the aromatic proton ($H_d$) in A-ring. Lithiation process in purpurin was identified by waning of phenolic hydroxyl groups ($-OH_a$ and $-OH_c$), upfield shift of aromatic $H_d$ proton and downfield shift of $-OH_b$ signal (Figure 3a–e). In case of 1 : 1 ratio of purpurin with LiOAc, $-OH_b$ shifted downfield to δ 16.58 ppm and the $H_d$ proton shifted upfield to δ 5.65 ppm. Upon increasing the purpurin-LiOAc concentration to 1 : 2 ratio, the $-OH_b$ signal shifted downfield at δ 18.12 ppm, whereas $H_d$ shifted upfield to δ 5.58 ppm (Figures 3a, 3d, 3e). A similar trend was also observed in ELP-2, where $-OH_b$ proton shifted downfield to δ 18.19 ppm from δ 13.91 [ELP-1] and 11.58 ppm [pristine purpurin] (Figures 3a, 3b, 3c). Likewise, the $H_d$ proton shifted upfield to δ 5.55 ppm from δ 6.35 and 6.58 ppm in ELP-1 and in pure purpurin, respectively. The extreme downfield shifts of the enolic $-OH_b$ group is attributed to the α,β-unsaturated carbonyl conjugation. The extent of downfield shift depends on the equilibrium between the mono- and di-lithiated species. When the di-lithiated species dominate, the $-OH_b$ resonance has a maximum downfield of δ 18.14 ppm, which was observed in ELP-2 and chemically lithiated purpurin (1 : 2 ratio).

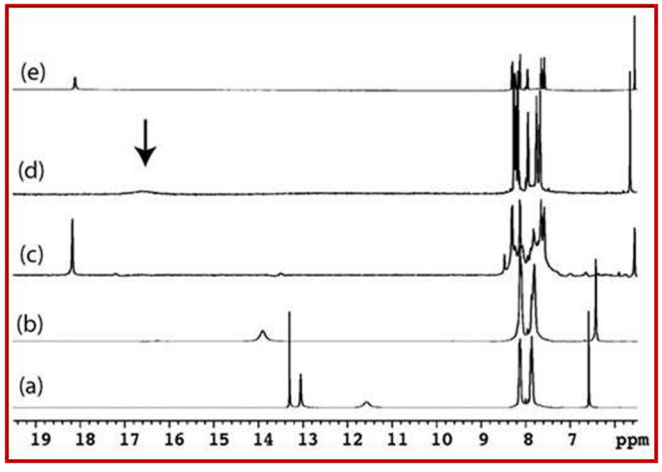


**Figure 3** | **The expanded $^{1}H$-NMR spectrum recorded in DMSO-$d_6$ at 500 MHz at 25°C.** (a) Pristine purpurin; (b) Lithiated purpurin electrode [ELP-1] (Cells were discharged (lithiated) from open circuit voltage to 1.5 V vs Li/$Li^+$ in 1 M solution of $LiPF_6$ in 1 : 1 (v/v) mixture of ethylene carbonate (EC) and dimethyl carbonate (DMC) as electrolyte); (c) Lithiated purpurin electrode [ELP-2] (Cells were discharged (lithiated) from open circuit voltage to 0.02 V in 1 M solution of $LiPF_6$ in 1 : 1 (v/v) mixture of EC and DMC as electrolyte) and (d) CLP using LiOAc as $Li^+$ source (1 : 1) and (e) CLP using LiOAc as $Li^+$ source (1 : 2).

The broadband decoupled $^{13}C$ NMR spectrum of purpurin exhibited carbonyl carbon peaks at around δ 181 and 188 ppm and the carbon attached to hydroxyl group appeared at δ 150, 158 and 161 ppm. Depending on the extent of lithiation, the carbonyl carbons displayed slight upfield shifts, whereas the aromatic carbons attached to the hydroxyl group exhibited downfield shifts (Figure S2). Figure 4a–d display the overlayed $^{13}C$-DEPT-135 spectra of pristine purpurin, ELP-1, ELP-2 and CLP, where only the proton bearing carbons are detected. Strikingly, the $C_d$ carbon shifted upfield from 110.3 ppm in pure purpurin to 104.4 ppm, depending on the extent of lithiation process. In addition, the observations from $^{1}H$ and $^{13}C$ NMR are further supported by $^{7}Li$ NMR as shown in Figure S3.

The Lithiation process in purpurin was further substantiated by UV/VIS and FTIR analysis. Optical absorption spectra of purpurin ($1\times10^{-4}$ M) upon titration with $Li^+$ ($1\times10^{-4}$ M) indicated some absorbance changes in UV/vis region (Figure 5a). Lithiation of

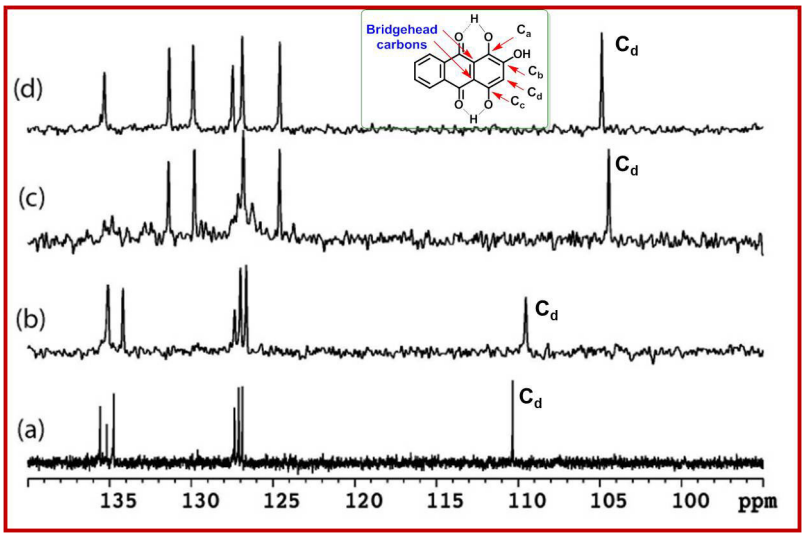


**Figure 4** | **The expanded $^{13}C$ DEPT-135 NMR spectrum recorded in DMSO-$d_6$ at 125 MHz at 25°C.** (a) Pristine purpurin; (b) ELP-1; (c) ELP-2 and (d) CLP (1 : 2 ratio). In DEPT 135, $^{13}C$ signals arising due to methyl ($-CH_3$) & methine (–CH) appear positive, methylene as negative ($-CH_2$) whereas no quaternary carbons show up. The progress of lithiation and its corresponding carbon chemical shifts were examined. The inset shows the molecular structure of purpurin with carbon labeling as $C_a$–$C_d$ respectively.

purpurin leads to the decrease in the absorption in the region of 481 nm with red shift of absorption band from 481 to 487 nm. In addition, appearance of a new band at 514 nm was observed and it was enhanced with the subsequent addition of $Li^+$ ions. Once it reached the ratio of 1 : 2 purpurin to lithium, no amendment in absorption was perceived (Figure 5a). FTIR analysis of ELP-1 showed new carbonyl stretching absorption bands at around 1780 and 1800 $cm^{-1}$, whereas they were absent in the case of pristine purpurin (Figure 5b). Further, solid product obtained after several cycles of charge/discharge process was characterized using a PHI Quantera photoelectron spectrometer (XPS) with an Al anode source operated at 15 kV and an applied power of 350 W. Lithiated purpurin samples after last discharge was load locked into the XPS machine without exposing it to ambient air. XPS profiles were analyzed by focusing on the regions where the signals of C1s, O1s and Li1s are expected and compared with that of pristine purpurin (Supporting information Figure S4). The XPS survey scan is shown Figure S4, which specifies the presence of both carbon and oxygen similar to that of purpurin (Supporting information Figure S4) and an additional peak at a binding energy of ~55 eV the presence of lithium in the sample. Further, the core level spectra of Li1s is also obtained by focusing the region corresponding to Li1s signal and presented as inset in Figure S5. The corresponding C1s and O1s core levels in lithiated purpurin are shown in supporting information Figure S6. The Li1s core level spectra has been corrected for any background signals using the Shirley algorithm prior to curve resolution and then resolved into two components centered at ~54.8 and 56 eV as shown in inset of Figure S5. The lower binding energy component centered at 54.8 eV confirms the formation of –OLi in the coordination compound and the higher binding energy component centered at 56 eV corresponds to lithium oxide, which may be due to an impurity left in the purpurin sample.

## Discussion

We have explored chemical and electrochemical reversible lithium ion properties and understood the reaction mechanism in purpurin molecule. Reversible lithiation/de-lithiation process in purpurin electrode is observed from electrochemical studies (Figure 1). Observed anodic peak at 2 V and cathodic peaks ~2.6 and 3.2 V from cyclic voltammetry studies are clear evidence of reversible lithiation/de-lithiation process in purpurin molecule. Similar Galvanostatic charge/discharge behavior observed in purpurin and CLP is a clear indication that CLP can alone stand as cathode material. The reversible capacity of 90 mAh/g obtained after 50 charge/discharge

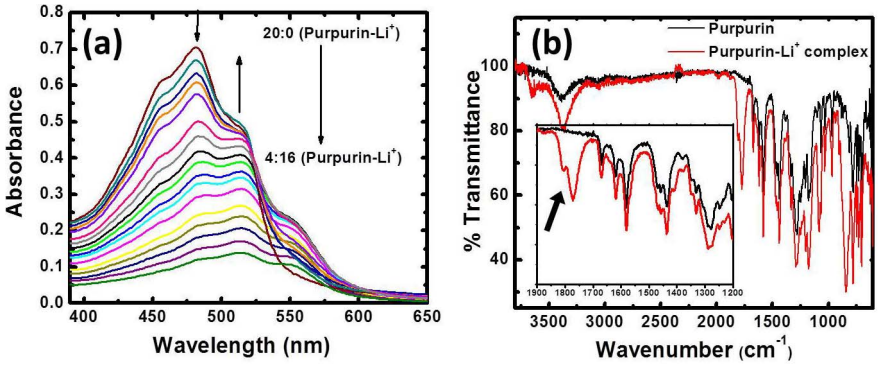


**Figure 5** | (a) UV/vis absorption titration curves of purpurin ($1\times10^{-4}$ M) with addition of LiOAc ($1\times10^{-4}$ M) in methanol at 298 K. The ratio of purpurin with LiOAc was changed throughout the titration in different ratios, starting from 20 : 0 to 4 : 16 (top to bottom), and change in absorption curves were pointed out by arrows and (b) FT-IR (ATR) spectrum of purpurin (black) and ELP-1 (red). The inset shows an expanded view, where the existence of new absorption bands for carbonyl groups is clearly visible and point out by arrow.

cycles in purpurin is comparable to conventional inorganic insertion cathodes such as $LiCoO_2$ or $LiFePO_4$ and also with recently studied other organic compounds such as $Li_2C_6O_6$ and $Li_2C_6H_4O_4$[5,21–23]. We believe that the specific capacities and rate capabilities of these low electron conducting organic molecules can be further improved by using specially engineered current collectors reported in reference number 29 and 30. Further, proposed mechanism in Figure 2a and existence of different molecular forms of purpurin are based on detailed NMR, FTIR, UV and XPS studies. Thorough NMR studies on both CLP and ELP molecules at various stages of lithiation process supports the binding of $Li^+$ ions with carbonyls and simultaneously with the nearby hydroxyl groups of purpurin as shown in Figure 2A. It should be noted that purpurin and its lithiated analogues have different levels of CH ($sp^3$) character of the bridgehead carbons. The formation of most favored six membered co-ordination site optimize the lithiation process and further increases the capacity of the purpurin-based electrodes.

To conclude, we have demonstrated reversible lithiation/de-lithiation properties in purpurin molecules that is derived from a widely available plant Madder. The lithium batteries assembled using purpurin and chemically lithiated purpurin as working electrodes showed good charge/discharge characteristics with a reversible capacity of ~90 mAh/g. The chemistry behind the lithiation of purpurin molecule was studied with NMR, UV and FTIR. We demonstrate that the binding of two lithium ions with purpurin molecule by the shared binding of carbonyl and nearby hydroxyl group, lead to the formation of most favored six membered structure. Our results pay a way towards the development of green and sustainable lithium battery electrodes from plant/crop-based materials[24] and agricultural wastes.

## Methods

**Synthesis of chemically lithiated purpurin.** Pristine purpurin was chemically lithiated by following the basic lithiation chemistry procedures reported in the literature[26–28]. Lithium acetate dihydrate (1.02 g, 10 mmol) in 10 mL of MeOH was added drop-wise to a solution of purpurin (2.56 g, 10 mmol) dissolved in 100 mL of methanol. During the addition of LiOAc solution, reddish yellow colored purpurin solution turned to pink, and the resultant solution was stirred vigorously for 10 minutes. The 1 : 1 ratio of chemically lithiated purpurin (CLP) was obtained by removing the solvent from the reaction mixture and by drying the solid product under vacuum. Similar procedure was followed for the preparation of 1 : 2 ratio of CLP, by increasing the molar equivalent of LiOAc twice.

**Electrochemical characterization.** Cyclic voltammograms were performed in a Swagelok-type cell using *AUTO LAB PGSTAT 302* potentiostat/galvanostat (Eco Chemie Utrecht, Netherlands) and galvanostatic charge/discharge measurements were conducted using an Arbin battery analyzer (USA). The working electrode with a thickness of 0.2 mm and a diameter of 12 mm was fabricated by mixing 80% of the active materials with 20% carbon black and coated onto a stainless steel (SS) plate. The electrochemical test cells were assembled in an argon-filled glove box using the active material (purpurin and CLP) as working electrode, lithium metal foil as the counter/reference electrode and 1 M solution of $LiPF_6$ in 1 : 1 (v/v) mixture of ethylene carbonate (EC) and dimethyl carbonate (DMC). A glass microfiber filter was used as separator. The cell charge/discharge was performed between 3.7 V and 1.5 V vs $Li/Li^+$ at different current rates.


1. Mann, M. E., Bradley, R. S. & Hughes, M. K. Global-scale temperature patterns and climate forcing over the past six centuries. *Nature* **779**, 779–787 (1998).
2. Mann, M. E., Zhang, Z., Hughes, M. K., Bradley, R. S., Miller, S. K., Rutherford, S. & Ni, F. Proxy-based reconstructions of hemispheric and global surface temperature variations over the past two millennia. *Proc. Natl. Acad. Sci. U.S.A.* **105**, 13252–13257 (2008).
3. Armaroli, N. & Balzani, V. The future of energy supply: challenges and opportunities. *Angew. Chem.* **46**, 52–66 (2007).
4. Armand, M. & Tarascon, J. M. Building better batteries. *Nature* **451**, 652–657 (2008).
5. Whittingham, M. S. Lithium batteries and cathode materials. *Rev. Chem.* **104**, 4271–4301 (2004).
6. Van Schalkwijk, W. & Scrosati, B. *Advances in Lithium-ion batteries* (Kluwer Academic/Plenum, New York, 2002).
7. Mizushima, K., Jones, P. C., Wiseman, P. J. & Goodenough, J. B. $Li_xCoO_2$ ($0<x<-1$): a new cathode material for batteries of high energy density. *Mater. Res. Bull.* **B15**, 783–789 (1980).
8. Thackeray, M. M., David, W. I. F., Bruce, P. G. & Goodenough, J. B. Electrochemical extraction of lithium from $LiMn_2O_4$. *Mat. Res. Bull.* **18**, 461 (1983).
9. Recham, N., Chotard, J. N., Dupont, L., Delacourt, C., Walker, W., Armand, M. & Tarascon, J. M. A 3.6 V lithium-based fluorosulphate insertion positive electrode for lithium-ion batteries. *Nature Mater.* **9**, 68–74 (2010).
10. Rao, C. V., Reddy, A. L. M., Ishikawa, Y. & Ajayan, P. M. $LiNi_{1/3}Co_{1/3}Mn_{1/3}O_2$–graphene composite as a promising cathode for Lithium-ion batteries. *ACS Appl. Mater. Interfaces* **3**, 2966–2972 (2011)
11. Lupi, C., Pasquali, M. & DelliEra, A. Nickel and cobalt recycling from lithiumion batteries by electrochemical processes. *Waste Manage* **25**, 215–220 (2005).
12. Novak, P., Muller, K., Santhanam, S. V. & Hass, O. Electrochemically active polymers for rechargeable batteries. *Chem. Rev* **97**, 207–282 (1997).
13. Heinze, J. Electronically conducting polymers. *Top. Curr. Chem.* **152**, 1–47 (1990).
14. Scrosati, B., Ed. *Application of electroactive polymers* (Chapman & Hall: London, 1993).
15. Caja, J., Kaner, R. B. & MacDiarmid, A. G. A rechargeable battery employing a reduced polyacetylene anode and a Titanium disulfide cathode. *J. Electrochem. Soc.* **131**, 2744–2750 (1984).
16. Armand, M. B. Utilization of conductive polymers in rechargeable batteries. In: Sequeira, C. A. C. & Hooper, A. (eds). *Solid state batteries.* Martinus Nijhoff Publ., Dordrecht, 1985; pp 363.
17. Passiniemi, P. & Osterholm, J. E. Critical aspects of organic polymer batteries. *Synth. Met.* **18**, 637–644 (1987).
18. Gowda, S. R., Reddy, A. L. M., Zhan, X. & Ajayan, P. M. Building energy storage device on a single nanowire. *Nano Lett.* **11**, 3329–3333 (2011).
19. MacDiarmid, A. G., Yang, L. S., Huang, W. S. & Humphrey, B. D. Polyaniline: electrochemistry and application to rechargeable batteries. *Synth. Met.* **18**, 393–398 (1987).
20. Qu, J., Katsumata, T., Satoh, M., Wada, J., Igarashi, J., Mizoguchi, K. & Masuda, T. Synthesis and charge/discharge properties of polyacetylenes carrying 2,2,6,6-tetramethyl-1-piperidinoxy radicals. *Chem. Eur. J.* **13**, 7965–7973 (2007).
21. Chen, H., Armand, M., Demailly, G., Dolhem, F., Poizot, P. & Tarascon, J. M. From biomass to a renewable $LiXC_6O_6$ organic electrode for sustainable Li-ion batteries. *Chem. Sus. Chem.* **4**, 348–355 (2008).
22. Chen, H., Armand, M., Courty, M., Jiang, M., Grey, C. P., Dolhem, F., Tarascon, J. M. & Poizot, P. Lithium salt of tetrahydroxybenzoquinone: toward the development of a sustainable Li-ion battery. *J. Am. Chem. Soc.* **131**, 8984–8988 (2009).
23. Armand, M., Grugeon, S., Vezin, H., Laruelle, S., Ribière, P., Poizot, P. & Tarascon, J. M. Conjugated dicarboxylate anodes for Li-ion batteries. *Nat. Mater.* **8**, 120–125 (2009).
24. Vemula, P. & John. G. Crops: a green approach toward self-assembled soft materials. *Acc. Chem. Res.* **41**, 769–782 (2008).
25. John, G., Shankar, B. V., Jadhav, S. R. & Vemula, P. K. Biorefinery: a design tool for molecular gelators. *Langmuir* **26**, 17843–17851 (2010).
26. Seebach, D. Structure and reactivity of lithium enolates. From pinacolone to selective C-alkylations of peptides. Difficulties and opportunities afforded by complex structures. *Angew. Chemie. Int. Ed.* **27**, 1624–1654 (1988).
27. Nagarajan, S., Muthuvel, P. & Das, T. M. Facile one-pot synthesis of inden-1-ol derivatives. *Synlett***15**, 2163–2166 (2011).
28. Pocker, Y. & Spyridis, G. T. Modulation of tautomeric equilibria by ionic clusters. Acetylacetone in solutions of lithium perchlorate-Diethylether. *J. Am. Chem. Soc.* **124**, 10373–10380 (2002).
29. Gowda, S. R., Reddy, A. L. M., Zhan, X. & Ajayan, P. M. Nano-porous nanorod current collectors for 3D batteries. *Nano Letters.* **12**, 1198–1202 (2012).
30. Vlad, A., Reddy, A. L. M., Ajayan, A., Singh, N., Gohy, J. F., Melinte, S. & Ajayan, P. M. Flexible lithium-polymer batteries with Cu@Si core-shell nanowire composites anodes *Proc. Natl. Acad. Sci. U.S.A.* **109**, 15168–15173 (2012).


## Acknowledgments

ALMAR and PMA express their sincere gratitude to Army Research Office for providing the funding for this work. SN and GJ acknowledges the support from NSF-CBET and PSC-CUNY Awards.

## Author contributions

A.L.M.R. devised the original concept. A.L.M.R., G.J. and P.M.A. developed the experimental design. A.L.M.R., S.N., S.R.G., P.P., P.C. and S.R.J. performed research. M.D. contributed to discussions of results. A.L.M.R. wrote the first draft of the manuscript and all authors participated in manuscript revision.

## Additional information

**Supplementary Information** accompanies this paper at http://www.nature.com/scientificreports

**Competing financial interests**: The authors declare no competing financial interests.



**How to cite this article:** Reddy, A.L.M. *et al.* Lithium storage mechanisms in purpurin based organic lithium ion battery electrodes. *Sci. Rep.* **2**, 960; DOI:10.1038/srep00960 (2012).